

Reconstruction of a distribution from a finite number of its moments: a comparative study in the case of depolymerization process

Noureddine Lebaz^{a,b,c,d,*}, Arnaud Cockx^{b,c,d}, Mathieu Spérandio^{b,c,d}, Jérôme Morchain^{b,c,d}

^aToulouse White Biotechnology (UMS INRA/INSA/CNRS), 3 rue Ariane, 31520 Ramonville Saint Agne, France

^bUniversité de Toulouse; INSA, UPS, INP; LISBP, 135 Avenue de Rangueil, F-31077, Toulouse, France

^cINRA, UMR792 Ingénierie des Systèmes Biologiques et des Procédés, F-31400, Toulouse, France

^dCNRS, UMR5504, F-31400, Toulouse, France

Abstract

The resolution of the Population Balance Equation (PBE) using moment-based methods offers a high computational efficiency however, information on the time evolution of the probability density function (PDF) is out of reach. For this, several PDF reconstruction methods using a finite number of moments are proposed in the literature. In this contribution, three different methods (i.e. Beta Kernel Density Function based method, Spline based technique and the Maximum Entropy based approach) are tested and compared to the analytical solution of a depolymerization process. The Maximum Entropy method gives the most accurate approximations using only a set of six moments. This method is combined with the Quadrature Method of Moments (QMOM) for a simultaneous reconstruction during the PBE resolution. A three nodes and a four nodes quadrature are tested. The results show that the quality of the reconstruction is highly dependent on the accuracy of the computed moments.

Keywords: Moment problem, population balance, reconstruction methods, maximum entropy

1. Introduction

The recovery of a probability density function (PDF) knowing only a finite number of its moments is known as the finite-moment problem in mathematical analysis and arises in different scientific applications (e.g. physics, chemical engineering, economics) (Gavriliadis & Athanassoulis, 2012; John et al., 2007). This problem is generally declined in three different problem categories for the mono-variate case (Abramov, 2007):

- The *Hausdorff* moment problem: the PDF is supported on the closed interval $[a, b]$
- The *Stieltjes* moment problem: the PDF is supported on $[0, +\infty)$
- The *Hamburger* moment problem: the PDF is supported on the real line $(-\infty, +\infty)$

In chemical engineering, especially for particulate/dispersed systems (e.g. crystallization, polymerization/depolymerization, liquid-liquid extraction, multiphase systems), population balance models (PBM) are

*Corresponding author. Address: INSA, LISBP, 135, avenue de Rangueil, F-31077 Toulouse, France. Tel.: +33 56 155 9798; Fax: +33 56 155 9760

Email address: lebaz@insa-toulouse.fr (Noureddine Lebaz)

widely used for the description of the time evolution of the variable-based distribution (e.g. size, volume) undergoing elementary processes. Among these processes, one commonly finds breakage, aggregation/coalescence, nucleation, growth/dissolution . . . etc (Ramkrishna & Mahoney, 2002). The resolution of the population balance equation (PBE) is computationally intensive when using classical approaches (e.g. Monte Carlo methods (Lin et al., 2002), discretization methods (Kumar & Ramkrishna, 1996)). This drawback is limiting when population balance modelling is coupled with Computational Fluid Dynamics (CFD) which is the case for multiphase systems. In order to overcome this issue, moment based methods (MOM: Standard Method of Moments (Hulburt & Katz, 1964), QMOM: Quadrature Method of Moments (McGraw, 1997; Marchisio et al., 2003a), DQMOM: Direct Quadrature Method of Moments (Marchisio & Fox, 2005)) have been developed. The problem is reduced to the time-tracking of a finite number of the PDF moments offering by the fact a high computational efficiency. In QMOM the transported moments are calculated by reducing the PDF to an n -point distribution (sum of n weighted Dirac delta functions), the corresponding weights and abscissas are computed using specific algorithms (John & Thein, 2012). In DQMOM, the weights and the abscissas of the initial n -point distribution are directly tracked instead of the moments.

Even though the moment-based methods are computationally efficient, information regarding either the shape or pointwise values of the PDF are identically out of reach. However, this level of knowledge is important for different applications as in the case of evaporation process where one needs to accurately evaluate the PDF at zero size (Massot et al., 2010) or in the enzymatic hydrolysis of particulate substrates where the loss of small solubilized particles produced by the enzymatic attacks has to be taken into account (Lebaz et al., 2015). To address this issue, different numerical techniques have been proposed for the reconstruction of the PDF from its moments reviewed by John et al. (2007), mainly for the Hausdorff moment problem since in chemical engineering applications, the support of the PDF is known in most cases.

From a mathematical point of view, the moment problem has been extensively studied focusing on the conditions of existence of a unique or infinite solution(s) (Shohat & Tamarkin, 1943; Akhiezer, 1965; Dette, 1997). Theoretically, a perfect reconstruction can be obtained using an infinity of PDF moments with an *a priori* restriction of the class of basis functions (John et al., 2007). Numerically, this problem is known as a difficult inverse problem since the finite number of moments define a high ill-posed system of equations (Athanasoulis & Gavriladis, 2002). Thus, there is no absolute method for reconstructing accurately the PDF from a finite number of its moments. From an experimental point of view the number of moments that can be obtained with a reasonable accuracy is limited.

The most intuitive reconstruction technique is to approximate the target PDF by a sum of elementary distributions (e.g. Gaussian, log-normal) (Lee, 1983; Diemer & Olson, 2002) when an information on the shape of the PDF is available *a priori*. Thus, the problem is reduced to a simple parameter fitting. This technique offers some advantages like the reduced number of moments required for the reconstruction, its simplicity and fastness but the shape of the target PDF has to be stipulated. This constitutes its principal limitation when the initial shape of the PDF changes dramatically during the course of the process. Inspired by this

approach, Athanassoulis & Gavriiadis (2002) proposed a robust technique based on the PDF approximation by a finite superposition of kernel density functions (KDF) for the *Hausdorff* moment problem, tested and validated successfully against both monomodal and bimodal PDFs. This approach has been extended for the *Stieltjes* moment problem using a generalized Gamma function as the kernel density function (Gavriiadis & Athanassoulis, 2012, 2009) but unfortunately it was not confronted to realistic cases.

John et al. (2007) proposed an innovative technique using a piecewise polynomial function without any *a priori* assumption about the shape of the target PDF. Linear, quadratic or cubic splines can be used, their coefficients are computed by solving an ill-conditioned linear system of equations. De Souza et al. (2010) improved the spline-based method by developing an adaptive algorithm in order to optimize the distribution of the grid nodes and capture more accurately the PDF in critical domains. This technique has been coupled recently with a PBE describing aggregation of urea particles (Hackbusch et al., 2012), droplet coalescence (Bordás et al., 2012) and pharmaceutical drying process (granules) (Mortier et al., 2014).

The third class of methods that will be considered in this paper is the Maximum entropy (ME) method which received increasing interest in the last two decades (Mead & Papanicolaou, 1984; Tagliani, 1999, 2001; Biswas & Bhattacharya, 2010). This technique is based on the maximization of the Shannon entropy from information theory, by solving a constraint optimization problem. Abramov (2006) extended it to multi-dimensional problems. Massot et al. (2010) coupled this technique with DQMOM in the case of droplet evaporation process.

In this paper we propose firstly an assessment of these methods in terms of accuracy, rapidity and minimum number of moments required for the reconstruction. The issue concerns the identification of the most efficient method to perform the reconstruction throughout the process (not only for a particular distribution). The performances of the three methods will be evaluated through a comparison of the reconstructed PDFs with an analytical solution of the PBE accounting for a breakage process. Finally, the implementation of the relevant method in the QMOM code for a simultaneous resolution of the PBE and reconstruction of the PDF is investigated. The outlines of this contribution are schematically summerized in figure 1.

2. Reconstruction methods

The purpose of the reconstruction techniques is to recover a function $f(x)$, given its integer moments sequence μ_n defined as:

$$\mu_n = \int x^n f(x) dx, \quad n = 0, 1, \dots \quad (1)$$

We give hereafter a succinct description of the reconstruction techniques used in this contribution. For more detail, one can refer to the original works cited and/or to Appendix A. As common point, the bounded support $[a,b]$ is rescaled to $[0,1]$ for a general formulation.

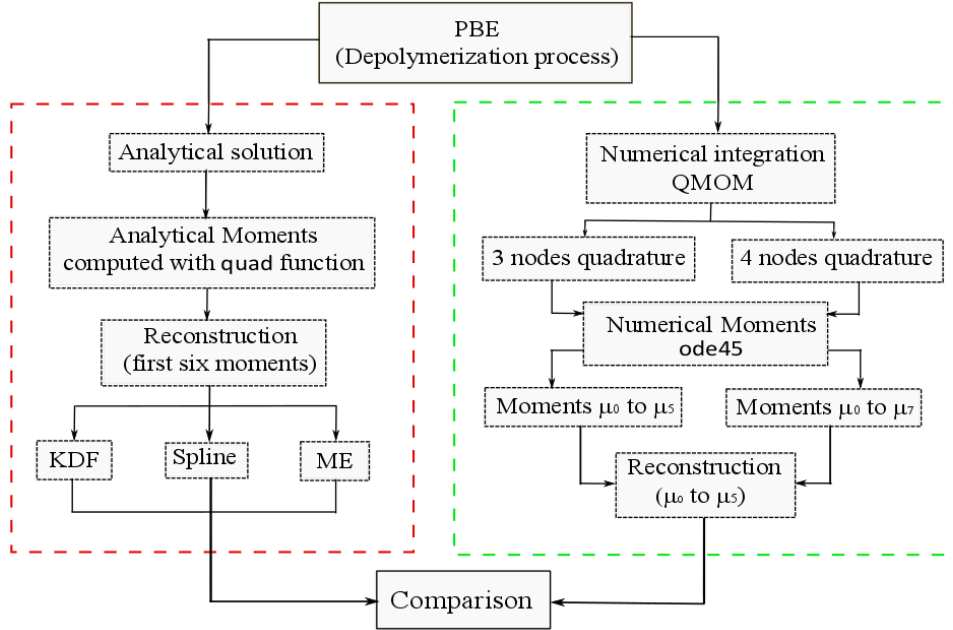


Figure 1: Schematic representation of the organigram of the contribution

2.1. Kernel Density Function-based method

In the KDF based technique, the target PDF is approximated by a sum of weighted kernel density
 80 functions (equation 2) (Athanasoulis & Gavriiladis, 2002):

$$f(x) = \sum_{i=1}^I p_i K(x; x_i, h) \quad (2)$$

where $K(x; x_i, h)$ are the KDFs, centered at x_i , with bandwidth h , I is the total number of kernel density functions used for the reconstruction. The coefficients p_i satisfy:

$$p_i \geq 0, \quad i = 1, 2, \dots, I; \quad \sum_{i=1}^I p_i = 1 \quad (3)$$

Since the target PDF is univariate, the KDF is chosen as a Beta Kernel. Thus, the objective is the deter-
 mination of the optimal coefficients p_i . For this, the finite-moment problem is reformulated as a constrained
 85 optimization problem aiming to find the coefficients p_i which minimize the error between the set of initial moments and those estimated via the sum of Beta KDFs. Numerically, Nonnegative Least Square algorithm (NNLS) can be used in this case. Optimization techniques are to be supplemented in order to improve the efficiency of this procedure. The properties of the Beta Kernel Function, the formulation of the constrained optimization problem, the optimization technique based on the shifted moments and the general algorithm

90 of this method are described in Appendix A.1.

2.2. Spline-based method

This method is extensively described by John et al. (2007). The support of the target PDF $[a, b]$ is subdivided into n subintervals such as $a = x_1 < x_2 < \dots < x_{n+1} = b$. In each subinterval $[x_i, x_{i+1}]$, the target PDF is approximated by a piecewise polynomial $s^{(l)}(x)$ of degree l . The system of equations is detailed
 95 for cubic splines ($l = 3$). The unknowns are the four coefficients of the n splines. A smooth transition at the boundaries of the interval is assumed meaning that the PDF, its first and second derivatives are null at the boundaries, this gives 2×3 equations. The continuity of the splines, their first and second derivatives at the nodes provides $3(n - 1)$ equations. The remaining $(n - 3)$ equations are supplemented by the moments. This leads to solve a $4n \times 4n$ ill-conditioned linear system.

100 Since the set of the known moments limits the number of splines, one has to compute the reconstruction in the optimal support of $f(x)$ thus, the reconstruction is computed iteratively starting from an initial reconstruction $f^{(0)}(x)$ in an initial interval $[x_1^{(0)}, x_{n+1}^{(0)}]$. To ensure the positivity of the reconstructed PDF a tolerance tol_{neg} is introduced. Furthermore, the optimization of the distribution of the nodes improves the efficiency of the method especially for multimodal functions. More details on these techniques are given in
 105 Appendix A.2

2.3. Maximum Entropy method

The Maximum Entropy method is based on the maximization of the Shannon entropy $H[f]$ from information theory given by:

$$H[f] = - \int_0^\infty f(x) \ln f(x) dx \quad (4)$$

Under the moments constraints defined by equation 1.

110 The explicit representation of the ME approximation $f_M(x)$ of the target PDF takes the form:

$$f_M(x) = \exp \left[- \sum_{j=0}^N \xi_j x^j \right] \quad (5)$$

To be supplemented by the $(N + 1)$ constraints:

$$\mu_i = \int_0^\infty x^i f_M(x) dx \quad i = 0, 1, \dots, N \quad (6)$$

The $(N + 1)$ Lagrange's multipliers ξ_0, \dots, ξ_N are obtained through the resolution of the following set of $(N + 1)$ nonlinear equations:

$$\int_0^\infty x^i \exp \left[- \sum_{j=0}^N \xi_j x^j \right] dx = \mu_i \quad i = 0, 1, \dots, N \quad (7)$$

Numerically, iterative methods are used to solve equation 7 (Mead & Papanicolaou, 1984). In our case, we use the standard Newton method starting from an initial choice of the Lagrange's multipliers $\xi^{(0)}$ with a given tolerance for stopping the iterative procedure. Commonly used parameters are given in the results section.

3. Population balance modelling (PBM)

The mathematical modelling of polymer chain fragmentation processes (thermal, thermochemical and biological) is a fundamental issue in polymer science and engineering (McCoy & Madras, 2001; Bose & Git, 2004). Population balance modelling (PBM) is the classical approach since it describes the dynamical evolution of the Chain Length Distributions (CLD) (or MWD: Molecular Weight Distributions) during depolymerization reactions (Ziff & McGrady, 1985; Madras & McCoy, 1998).

For a homogeneous system, the time evolution of the CLD undergoing fragmentation processes is described by the population balance equation (PBE) below, written in its continuous form:

$$\frac{\partial n(L, t)}{\partial t} = \int_L^\infty \beta(L, L') \gamma(L') n(L', t) dL' - \gamma(L) n(L, t) \quad (8)$$

where $n(L, t)$ is the length-based number density function (CLD), $\gamma(L)$ the breakage frequency for a chain of length L , $\beta(L, L')$ is the breakage kernel giving the probability of obtaining a chain of length L from the breakup of a chain of length L' . The first term on the RHS accounts for the formation (birth) of chains with length L resulting from the breakage of longer chains L' . The last term is the death term due to the loss of chains of length L because of their breakup.

Except for some cases where analytical solutions exist, equation 8 is solved numerically. Since the resolution of this equation is not the objective of this contribution, an analytical solution is briefly described and used as reference for the moment problem.

3.1. Analytical solution of the PBE accounting for breakage process

Ziff & McGrady (1985) considered linear polymers of length L and gave the analytical solution of the equation 8 with the breakage kernel $\beta = 2/L$ and the breakage frequency $\gamma = \alpha L^2$ (α is a factor of proportionality) which can be regarded as the number of attacks per time unit. Under these considerations, equation 8 can be rewritten as:

$$\frac{\partial n(L, t)}{\partial t} = 2\alpha \int_L^\infty L' n(L', t) dL' - \alpha L^2 n(L, t) \quad (9)$$

The general solution of the equation 9 is given as (Ziff & McGrady, 1985):

$$n(L, t) = e^{-\alpha t L^2} \left(n(L, 0) + 2\alpha t \int_L^\infty L' n(L', 0) dL' \right) \quad (10)$$

140 where $n(L, 0)$ is the initial CLD.

In order to explicit this solution, we assume that the initial chain length distribution (CLD) follows a normal law (equation 11) with (m, σ) its mean and standard deviation respectively.

$$n(L, 0) = \frac{1}{\sigma\sqrt{2\pi}} e^{-\frac{(L-m)^2}{2\sigma^2}} \quad (11)$$

The explicit solution in this specific case is given as (details are given in Appendix B) :

$$n(L, t) = \frac{1}{\sigma\sqrt{2\pi}} e^{-\alpha t L^2} \left[(2\alpha t \sigma^2 + 1) e^{-\frac{1}{2} \left(\frac{L-m}{\sigma} \right)^2} + m \sigma \alpha t \sqrt{2\pi} \left(1 - \operatorname{erf} \left(\frac{1}{\sqrt{2}} \frac{L-m}{\sigma} \right) \right) \right] \quad (12)$$

where erf refers to the error function.

145 Thus, starting with a CLD following a normal law with specific fragmentation process, one can obtain the exact CLD and compute its moments at any given time during the degradation reaction.

3.2. The Monovariate Quadrature Method of Moment (QMOM)

The PBE's resolution using Moment Methods is based on the time tracking of a finite set of the CLD moments instead of the CLD itself. This class of methods is widely used for its low computational cost thus, 150 it can be implemented in CFD codes or extended to multidimensional problems. A succinct description of the well-known Quadrature Method of Moments (QMOM) proposed by McGraw (1997) and validated by Marchisio et al. (2003b) is given in the specific case of breakage processes.

By a moment transformation of equation 8, the transport equation for the k^{th} moment is:

$$\frac{\partial \mu_k(L, t)}{\partial t} = \int_0^\infty L^k \int_0^\infty \gamma(L') \beta(L, L') n(L', t) dL' dL - \int_0^\infty L^k \gamma(L) n(L, t) dL \quad (13)$$

155 The Quadrature Method of Moments (QMOM) is based on the Gaussian quadrature of the continuous CLD (McGraw, 1997):

$$n(L, t) \approx \sum_{i=1}^M w_i(t) \delta(L - L_i(t)) \quad (14)$$

where M is the number of nodes i , L_i is the property of the node (length), w_i its weight, and δ is the Dirac function. Thus, the k^{th} moment can be expressed as :

$$\mu_k(t) = \int_0^\infty n(L) L^k dL \approx \sum_{i=1}^M w_i(t) L_i^k(t) \quad (15)$$

where weights (w_i) and abscissas (L_i) are determined through the Product-Difference algorithm (Gordon, 1968). By substituting equations 14 and 15 in 13, we obtain (Marchisio et al., 2003b) :

$$\frac{\partial \mu_k}{\partial t} = \sum_{i=1}^M \gamma_i \bar{b}_i^{(k)} w_i - \sum_{i=1}^M L_i \gamma_i w_i \quad (16)$$

160 with

$$\bar{b}_i^{(k)} = \int_0^\infty L^k \beta(L, L_i) dL \quad (17)$$

Generally, the QMOM requires at least a three nodes quadrature ($M = 3$) for an accurate time-tracking of the moments (Marchisio et al., 2003b).

MATLAB is used under a work-station comprising of an Intel[®] Core[™]i7-3740QM CPU with a clock speed of 2.7 GHz and 16 GB of installed memory (RAM).

165 4. Results and discussion

The reasons for searching efficient reconstruction techniques when one deal with solving PBM are multiple. First of all, Methods of Moments are rather powerful in terms of numerical performance but since these are integral methods the connection with the physical distribution (Chain Length Distribution or Molecular Weight Distribution) is lost. Moreover, high order moments of an experimental distribution are often hard to evaluate and the direct comparison of numerical and experimental moments remains difficult to analyze. In some cases, the distribution itself is necessary to evaluate some terms in the equations. To finish with, experimental and numerical distributions are not always known over the same range: the range of experimental methods is limited by lower and upper detection bounds. For all these reasons, an accurate reconstruction of a PDF from its moments is an essential tool for those involved in the analysis of experimental results with the help of mathematical models such as PBM solved with a method of moments.

4.1. Reconstruction of the analytical solution

As described before, the three reconstruction methods will be compared to the analytical solution given in section 3-1. We assume that the initial CLD is given by a normal law centered at a Degree of Polymerization (DP) of 60 (the mean number of monomers constituting a given polymer) with a standard deviation (σ) of 7. Equation 12 gives the time evolution of the CLD for ($\beta = 2/L$ and $\gamma = \alpha L^2$). This solution is illustrated in figure 2 with $\alpha = 10^{-3}$ and $t \in [t_i, t_f] = [0, 1]$.

Figure 2 shows a rapid degradation of the long polymers since the breakage frequency is proportional to L^2 , the concentration of the small polymer chains increases all along the depolymerization process.

For sake of clarity, the ability of the different methods to reconstruct the time evolution of the CLD is described separately and illustrated for five different instants: $t_0 = t_i$, $t_1 = \frac{1}{4}t_f$, $t_2 = \frac{1}{2}t_f$, $t_3 = \frac{3}{4}t_f$ and $t_4 = t_f$ before addressing a comparative analysis. At any given instant, the reconstruction is initiated by computing the set of the moments of the analytical CLD given in equation (12). The integrations leading to the associated moments, equation (1), are performed using the Matlab function *quad* with a tolerance set to 10^{-6} . Since the number of the moments required for the reconstruction is critical, the methods are tested with the same set of moments transformed systematically to the normalized interval $[0,1]$ before rescaling the reconstruction result (figure 1).

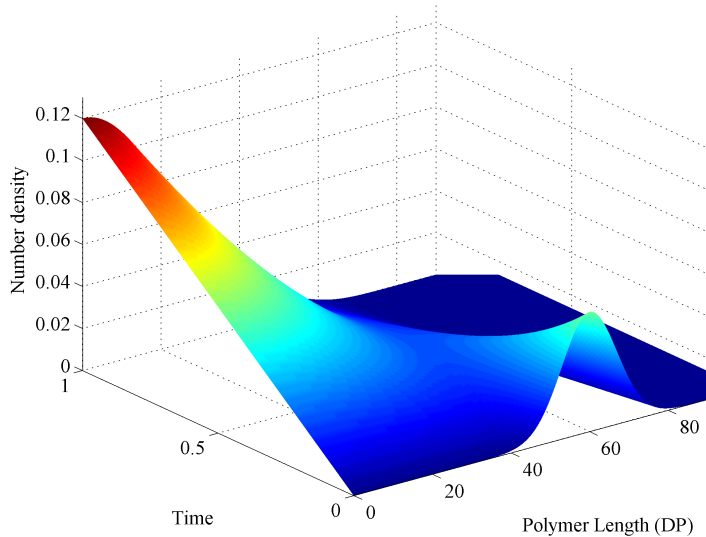


Figure 2: Time evolution of the CLD given by the analytical solution of Ziff & McGrady (1985)

In order to compare the different reconstruction methods, we introduce the mean absolute error between the reconstructed CLD ($f_M(x)$) and the analytical solution used as a reference ($f(x)$):

$$Er(t) = \frac{1}{q} \sum_{i=1}^q |f(x, t) - f_M(x, t)| \quad (18)$$

where q is the length of the discretized support.

195 4.1.1. Kernel Density Function-based method

The algorithm of this method was implemented in Matlab using the set of moments of each target CLD with their associated shifted moments by setting $\bar{x} = 0.8$ in order to increase the number of the constraints and thus improve the efficiency of this technique. The number of Beta Kernel Density Functions (BKDFs) I is set to 15 thus, the support $[0,1]$ is divided into 15 equal intervals, each BKDF is centered on the midpoint of
 200 its corresponding interval. Athanassoulis & Gavriliadis (2002) showed that the optimal bandwidth parameter h varies in the interval $[0.04,0.09]$. In order to identify the optimal values for h , the interval is scanned and the reconstruction is conducted at different parameter values before selecting the most accurate. Once the BKDFs parameters are fixed, the associated Beta PDF parameters are calculated and the coefficients $B_{n,i}$ and $\tilde{B}_{n,i}$ (equations A.3 and A.8) are computed. The constraint minimization problem (equation A.10) is
 205 solved using LSQLIN subroutine.

Figure 3 shows the results for the five different instants using the first six moments of each target CLD.

Although the initial CLD is reconstructed with great accuracy most probably because of its simple form, the other CLDs are not recovered. Their singular shape mainly around the origin makes their reconstruction challenging. The reconstructions are oscillating around the target CLDs and take the value zero at the origin.

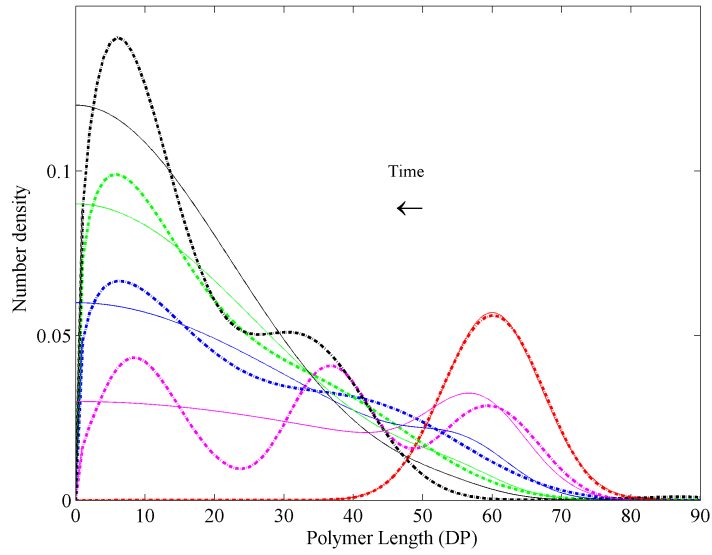


Figure 3: Comparison between the target CLDs (continuous line) and their reconstructions (dashed line) using the BKDF based technique with a sequence of six analytical moments

210 To be more accurate, this technique requires a large number of constraints which means a higher number of moments. In figure 4, the same problem is treated using the first eleven moments of each target CLD.

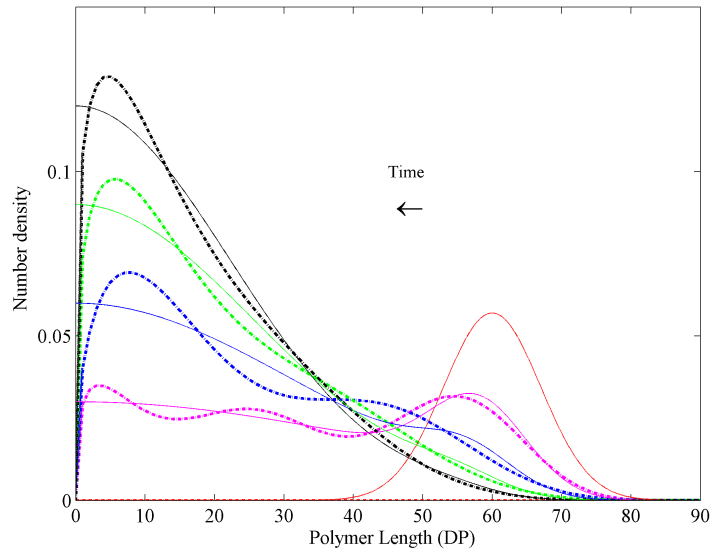


Figure 4: Comparison between the target CLDs (continuous line) and their reconstructions (dashed line) using the BKDF based technique with a sequence of eleven analytical moments

The figure 4 shows that the use of a high number of moments can improve the reconstruction quality

as illustrated in Table 1 where the mean absolute errors (equation 18) are calculated in both cases. But, since the technique is treating a highly ill-posed problem, the solution of the constraint system of equations may diverge. This is for example the case when the reconstruction of the initial CLD using eleven moments is attempted (figure 4). To sum up, this method requires a finetuning of the numerical parameters and an increase in the number of moments does not always guaranties an easier reconstruction. However if the reconstruction is successful, the accuracy increases with the number of moments.

Time	Mean absolute error	
	BKDF: 6 moments	BKDF: 11 moments
t_0	0.0002	/
t_1	0.0061	0.0014
t_2	0.0026	0.0033
t_3	0.0028	0.0024
t_4	0.0068	0.0023

Table 1: Reconstruction accuracy using the BKDF based technique with 6 and 11 moments

4.1.2. Spline-based method

The adaptive algorithm with cubic splines proposed by De Souza et al. (2010) is implemented and used in this contribution. The Matlab script for the original algorithm was freely downloaded from (<http://www.uni-magdeburg.de/isut/LSS>). The default tolerances proposed by the authors (tol_{red} and tol_{sing}) are kept unchanged. This procedure is adopted deliberately because when the reconstruction is conducted simultaneously with the PBE resolution, one has to set the parameters of the algorithm *a priori*. The authors recommended to set tol_{neg} at a very small negative value instead of 0. In our case, $tol_{neg} = -10^{-1}$ is used initially. The results of the reconstruction using the spline based method with six moments are shown in figure 5.

Only the initial CLD has been recovered using the parameters described before. For the other instants, the algorithm has been stopped after 10^3 iterations. The modification of the negative tolerance to $tol_{neg} = -5.10^{-3}$ leads to the convergence of the algorithm for t_1 but the reconstruction is highly oscillating. As mentioned by Mortier et al. (2014), the algorithm is highly sensitive to the negative tolerance leading to different reconstructions for the same target PDF as illustrated in figure 6. This is a main drawback since tol_{neg} may affect the algorithm and even its rate of convergence. In fact, for the example given in figure 6, the convergence is reached after 27 iterations for the case where $tol_{neg} = -10^{-1}$ when the algorithm needs 42 iterations for the second case ($tol_{neg} = -10^{-2}$).

Furthermore, a smooth transition at the boundaries of the reconstruction interval was assumed. This is the case only for the initial distribution thus, one has to change the boundary conditions during the process. This is not reachable without an *a priori* information on the shape of the target PDF.

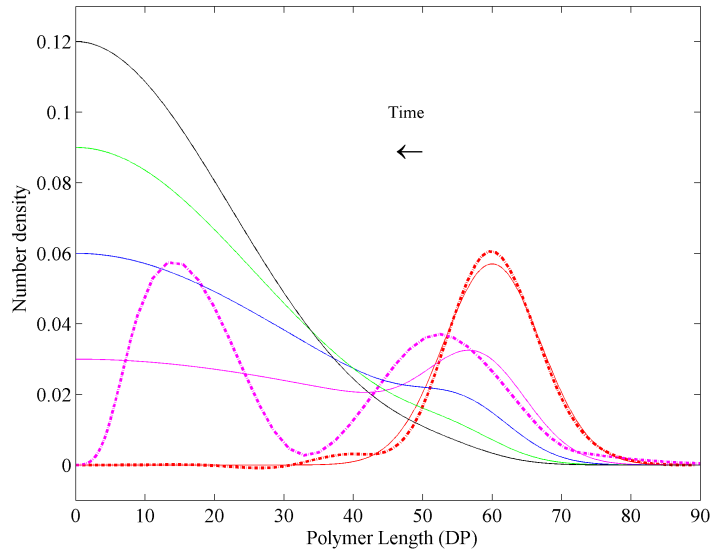


Figure 5: Comparison between the target CLDs (continuous line) and their reconstructions (dashed line) using the spline based technique with a sequence of six analytical moments

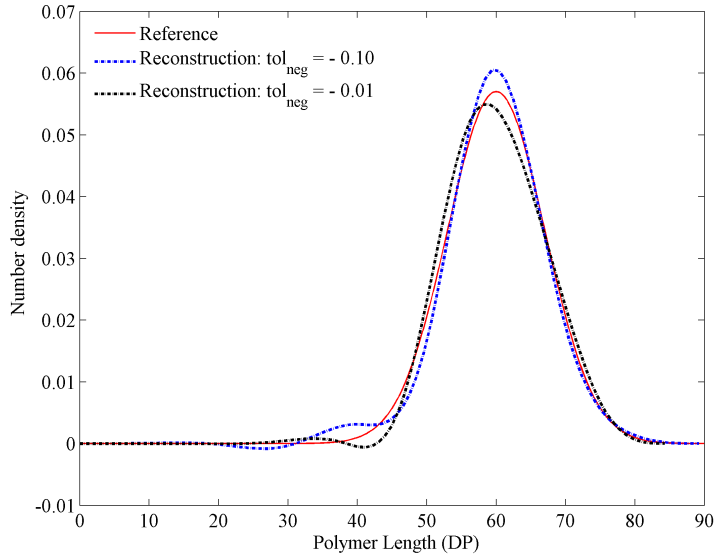


Figure 6: The sensitivity of the spline based method to tol_{neg}

4.1.3. Maximum Entropy based method

The non-linear system in equation 7 is solved using Newton method starting from an initial choice of the Lagrange's multipliers as $\xi^{(0)} = (-\ln(\mu_0)/(x_{max} - x_{min}), 0, \dots, 0)$ with a tolerance of 10^{-6} (Massot et al., 2010). The moments are scaled to $[0,1]$ and normalized before such as $\mu_0 = 1$. The results are given in figure

7.

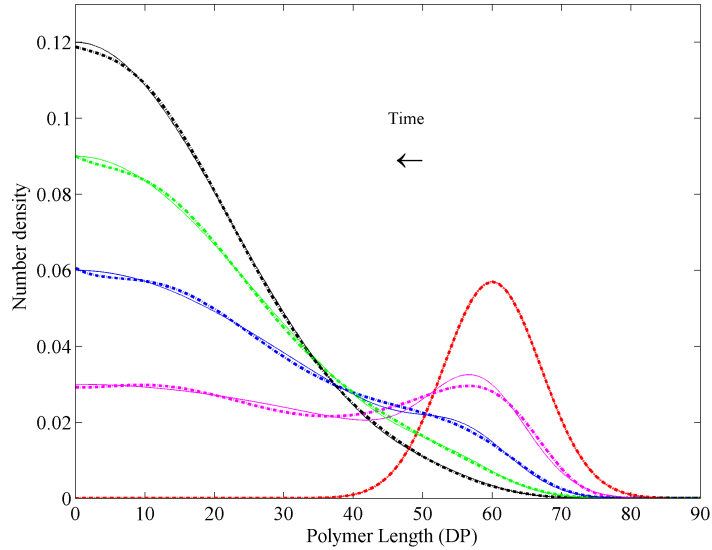


Figure 7: Comparison between the target CLDs (continuous line) and their reconstructions (dashed line) using the ME based technique with a sequence of six analytical moments

245 Unlike the two previous methods, the Maximum Entropy technique reconstructs the analytical CLDs with high accuracy even when they are singular using only the first six moments. The Newton method used in this case converges in a few iterations (< 10) making the coupling of the PBE resolution with the PDF reconstruction possible. In addition, except for the tolerance of the Newton method, there is no additional parameter to set which simplifies its use.

Time	BKDF based method		Spline based method		ME based method	
	Error	Cost (s)	Error	Cost (s)	Error	Cost (s)
t_0	0.0002	6.48	0.0011	6.48	0.0000	0.27
t_1	0.0061	6.47	0.0105	5.86	0.0008	0.26
t_2	0.0026	6.39	/	/	0.0005	0.23
t_3	0.0028	6.31	/	/	0.0004	0.20
t_4	0.0068	6.30	/	/	0.0004	0.20

Table 2: Comparison of the three different reconstruction methods (using the first six analytical moments) in terms of mean absolute error and computational cost

Table 2 gives the comparison between the three methods according to the quality of the reconstructed CLDs (mean absolute error) and the computational cost using the first six moments. The ME method gives

250 the best results for this case of study not only for the reconstruction efficiency but also for the number of moments required and the computational cost among other criterions as resumed in Table 3. For these reasons, this method is selected to be implemented in the QMOM code for coupling the PBE resolution in the case of depolymerization process with the CLD reconstruction.

Criterion	Beta KDF method	Spline-based method	ME based method
Principle	Approximation via a sum of kernel density functions	Approximation via connected peicewise polynomials	Approximation based on the maximization of Shannon entropy
Target PSD	No <i>a priori</i> information on its shape	No <i>a priori</i> information on its shape	No <i>a priori</i> information on its shape
Number of moments	> 10 to be accurate	Related to the number of intervals	Six or more
Computational cost	Acceptable	Acceptable when it converges	Very low
Robustness	The convergence is not guaranteed in all cases	The convergence is highly dependent on the parameters of the method	The convergence is guaranteed in most cases
Accuracy of the reconstruction	Depends on the number of moments, acceptable for simple shapes and oscillates for complex shapes	Highly oscillating results even for simple shapes, depends on the parameters of the method	Good occuracy even with just six moments, not affected by the parameters initialisation

Table 3: General comparison between the three different reconstruction methods

4.2. QMOM coupled with ME based method

255 The main objective of the development of reconstruction methods from a finite set of moments, especially in the chemical engineering field, is to have access to the shape of the PSD and/or some relevant pointwise values during the process evolution. This kind of information is necessary when some aspects of the problem cannot be expressed from the moments only. This offers a valuable addition when the PBE is solved using moment methods coupling by the fact the computational efficiency of such methods with a simultaneous
 260 information on the PDF shape.

In this section, the ME based method tested successfully against an analytical solution giving the time evolution of the CLD undergoing breakage process is implemented in the QMOM code resolving the same breakage problem. Thus, on the one hand, the analytical CLDs are available for comparison, on the other

hand, the PBE accounting for the same breakage process is solved using QMOM giving the time evolution of the moments which are used for the reconstruction (see figure 1).

For this numerical approach, a three nodes quadrature is used ($M=3$), the abscissas (L_i) and the weights (w_i) are computed using the Product-Difference algorithm (Gordon, 1968). The system of ordinary differential equations (equation 16) is integrated using *ode45* with a tolerance fixed to 10^{-6} . First, the QMOM implementation is validated by confronting the computed moments against those predicted by the analytical solution.

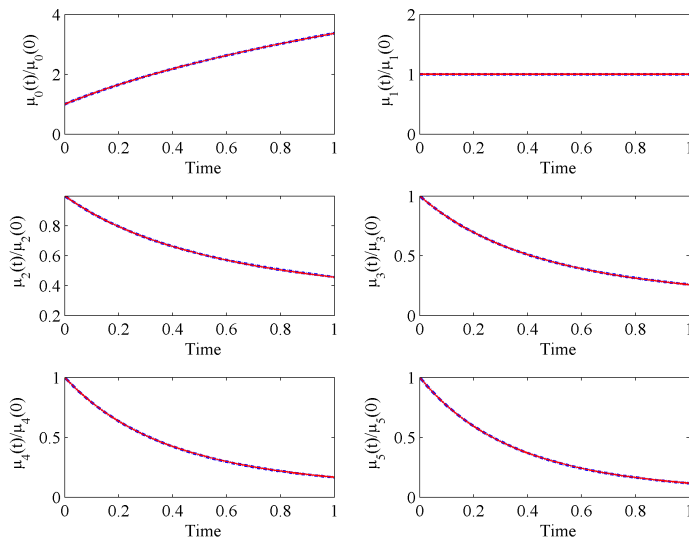


Figure 8: The time evolution of the six first moments: comparison between the analytical solution (continuous line) and QMOM with three nodes (dashed lines)

The results for the six first moments are given in figure 8. The two different methods lead to the same time evolution of the moments thus, the QMOM implementation is validated.

Since a three nodes quadrature is used, six moments are tracked. This set of moments is used as input for the ME based method. The reconstruction is conducted simultaneously with the PBE resolution. The result at different process time is shown in figure 9.

The reconstructions based on the numerical moments computed via QMOM (figure 9) are less accurate than those obtained previously with the exact analytical moments (figure 7). Note that the same number of moments is used in the two cases. This can only come from the numerical error introduced by QMOM. In order to improve the accuracy of the method, one can increase the number of the quadrature nodes. For quantifying the gain in terms of accuracy, we introduce the global error function below:

$$E(k) = \frac{|\mu_k - \mu_k^*|}{\mu_k^*} \quad (19)$$

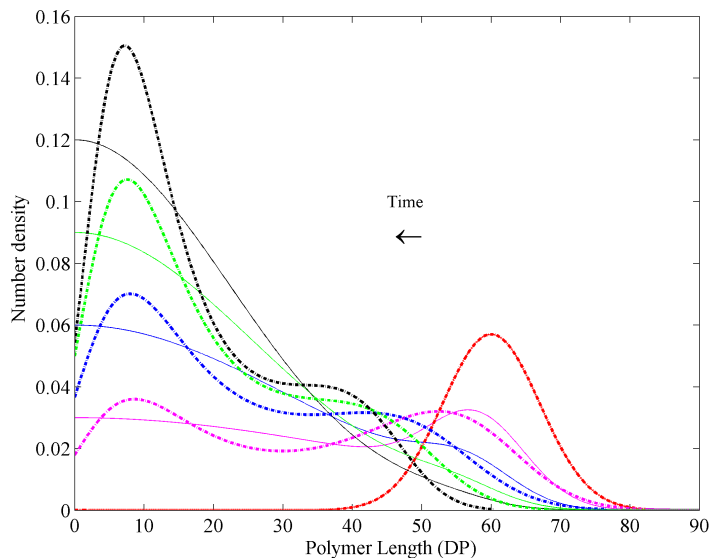


Figure 9: Comparison between the target CLDs (continuous line) and their reconstructions (dashed line) using the ME based technique with a sequence of six moments computed via QMOM with a three nodes quadrature

where μ_k is the k^{th} order moment estimated via QMOM and μ_k^* the exact k^{th} order moment calculated via the analytical solution.

We give in figure 10 the error $E(k)$ induced by QMOM for both a three and four nodes quadrature for the six first moments. Note that the use of a four nodes quadrature implies a time tracking of the first eight
 285 moments of the CLD.

The use of a four nodes quadrature in QMOM improves the accuracy of the computed moments, which constitutes a trivial and expected result. Note however that the use of a higher number of nodes induces supplementary moments meaning more equations in the system (equation 16) and may lead to near-singular matrix limiting the efficiency of PD algorithm.

Now, if the first six moments computed using a four nodes quadrature are used for the reconstruction,
 290 the result is completely different as shown in figure 11 and in Table 4.

Improving the accuracy of the tracked moments has considerably improved the reconstruction quality without reaching the same performance as with the analytical solution (figure 7). This shows that, if the ME based method is coupled with QMOM, one has to compute the moments with a high accuracy. For the
 295 reconstruction purpose, it is wise to track some additional moments in order to improve the accuracy of the set of moments that will be used.

To avoid the use of the PD algorithm for computing the weights (w_i) and the abscissas (L_i) all along the process which may introduce a subsequent error for the computed moments, the Direct Quadrature Method of Moments (DQMOM) presents an alternative (Marchisio & Fox, 2005). In this method, the PD algorithm
 300 is only called once, for initializing the quadrature nodes.

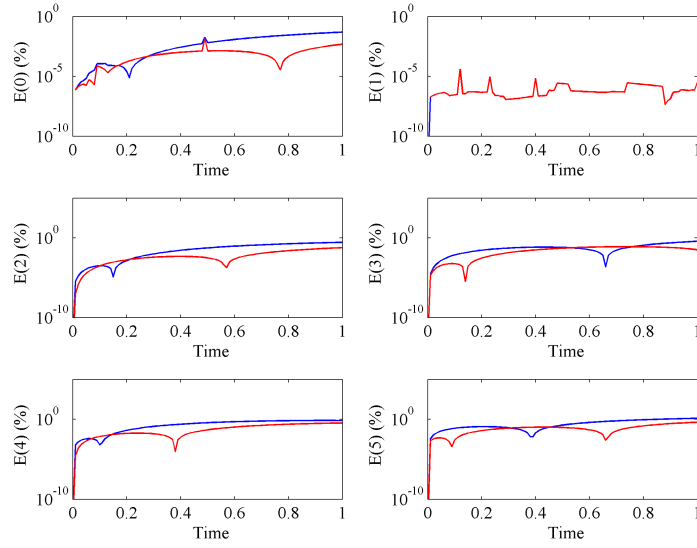


Figure 10: Comparison of the error induced by QMOM for the six first moments when using a three nodes quadrature (blue line) and a four nodes quadrature (red line)

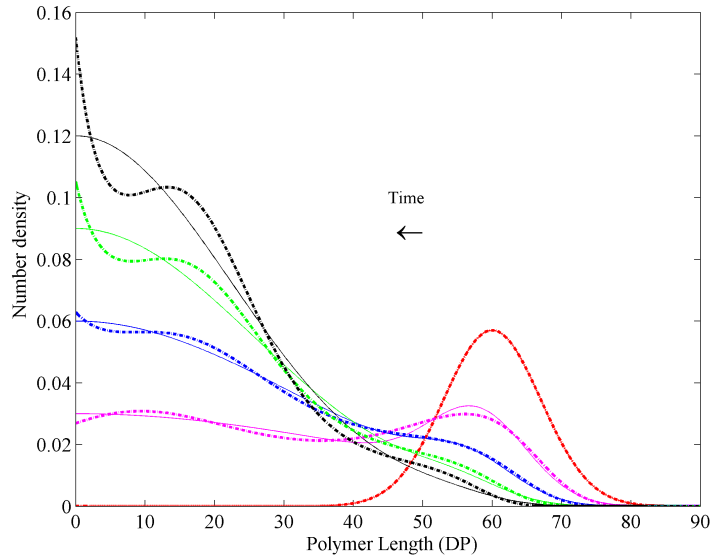


Figure 11: Comparison between the target CLDs (continuous line) and their reconstructions (dashed line) using the ME based technique with a sequence of six moments computed via QMOM with a four nodes quadrature

This method has been investigated and comparative results as with QMOM are obtained. The error on computing the initial (L_i, w_i) is transported throughout the process time. In addition, it has been shown that more accurate and robuste algorithms can be used instead of the PD algorithm for computing the nodes (John & Thein, 2012). The use of the Wheeler algorithm (called also LQMDA for Long Quotient-Modified

Time	Mean absolute error	
	QMOM-ME: M=3	QMOM-ME: M=4
t_0	0.0000	0.0000
t_1	0.0027	0.0010
t_2	0.0037	0.0007
t_3	0.0054	0.0019
t_4	0.0080	0.0031

Table 4: Reconstruction accuracy using the ME based technique with six moments: comparison between the use of the moments computed with a three nodes quadrature and those obtained with a four nodes quadrature

305 Difference Algorithm or Chebyshev algorithm) (Wheeler, 1974), recommended for computing optimal weights and abscissas (Yuan et al., 2012; John & Thein, 2012), leads to the same results as those shown before. So in the case studied here, combining DQMOM with the Wheeler algorithm does not seem to improve the accuracy of the reconstruction. The advantage of this algorithm is to avoid the limitation of the PD algorithm when near-singular matrix arise.

310 5. Conclusion

The reconstruction of a full PDF knowing only a finite/small number of its moments is of critical importance especially for particulate systems where information on the PDF shape is needed for process follow-up. Different reconstruction methods are available in literature but none of them is able to recover all the possible PDF shapes perfectly.

315 In this contribution, three different methods are investigated and their results confronted firstly against an analytical solution in the specific case of depolymerization process. The BKDF based method approximates the target PDFs by a finite sum of elementary Beta Kernel Density Functions and gives relative accurate results but requires a high number of moments for complex PDF shapes. The spline based method is highly dependent on the tolerance parameters. Finetuning of these parameters affects the rate of convergence of the algorithm and the final reconstructed PDF and depends on each single target PDF. Furthermore, the transition at the boundaries of the reconstruction interval has to be assumed which is not reachable when no information about the shape of the target PDF is available. As consequence, this method is not adapted for process monitoring when the distribution is needed at different time steps. The ME based method gives the best results and reconstructs the analytical target PDFs with high accuracy using only a set of six moments. 320 The method converges within a few iterations which makes it relevant to be coupled with the PBE resolution methods. This has been investigated in the second part.

Once the Quadrature Method of Moments accounting for breakage processes is validated against the analytical solution, the computed moments are used as inputs for the reconstruction method. The results

show that the ME based technique is highly dependent on the moments accuracy. When a three nodes
 330 quadrature is used for tracking the abscissas and the weights via the PD algorithm, the sets of associated
 moments lead to unsatisfactory reconstructions. Increasing the number of nodes improves significantly the
 moments accuracy and by the way the quality of the reconstruction. No doubt that the issue is common to
 all reconstruction methods: accurate values of the moments are required.

In summary, the ME based method is preferred than the BKDF and spline based methods because it
 335 requires a smaller number of moments and offers the best computational cost/reconstruction accuracy. The
 cases where a frequent reconstruction is needed along with the PBE resolution, the moments have to be
 computed accurately to achieve a good reconstruction quality using the ME based method. This is the main
 drawback when dealing with experimental moments. Further confrontation especially when different processes
 are coupled (e.g. breakage, aggregation, growth) is needed for assessing the relevance of this method.

340 Acknowledgments

The authors would like to thank *Toulouse White Biotechnology* and *Région Midi-Pyrénées* for their
 financial support.

Appendix A: Description of the reconstruction techniques

Appendix A.1: Kernel Density Function-based method

345 The Beta PDF is given, in its normalized form with κ and λ as parameters, by:

$$g(x; \kappa, \lambda) = \frac{\Gamma(\kappa + \lambda)}{\Gamma(\kappa)\Gamma(\lambda)} x^{\kappa-1} (1-x)^{\lambda-1}, \quad \kappa, \lambda > 0 \quad (\text{A.1})$$

where Γ is the *Gamma* function. The Beta kernel is then defined by :

$$K(x; x_*, h) = g(x; \kappa, \lambda) \quad (\text{A.2})$$

The Beta KDF parameters (x_* and h) are related to the Beta PDF parameters (κ and λ) (see Appendix
 A (Athanasoulis & Gavriiladis, 2002)).

The moments of the Beta kernel can be analytically calculated thanks to the equation A.3 :

$$B_n(x_*) = B_n(\kappa, \lambda) = \int_0^1 x^n g(x; \kappa, \lambda) dx = \frac{\Gamma(\kappa + \lambda)\Gamma(\kappa + n)}{\Gamma(\kappa)\Gamma(\kappa + \lambda + n)} \quad (\text{A.3})$$

350 By substituting equation A.3 in 2, one obtains the moments μ_n^* of the reconstructed distribution :

$$\mu_n^* = \sum_{i=1}^I B_{n,i} p_i, \quad n = 0, 1, \dots, N_1 \quad (\text{A.4})$$

For determining the unknown coefficients p_i , the finite-moment problem is reformulated as a constrained optimization problem (equation A.5):

$$\|\mu_n - \mu_n^*\|_{L^2} = \min, \quad \left(p_i \geq 0, \sum_{i=1}^I p_i = 1 \right) \quad (\text{A.5})$$

Equation A.5 can be solved numerically using a Nonnegative Least Square algorithm (NNLS). For improving the efficiency of this method and reducing the number of moments required for the reconstruction, different optimization techniques are available in literature such as the use, in addition of the given moments, of the shifted moments as described in the original work by (Gavriliadis & Athanassoulis, 2003).

The shifted moments of $f(x)$ are defined by:

$$\tilde{\mu}_n = \int_0^1 (x - \bar{x})^k f(x) dx, \quad n = 1, 2 \dots N_2 \leq N_1, \quad \bar{x} \in [0, 1] \quad (\text{A.6})$$

Since, in the finite-moment problem, $f(x)$ is the target, the shifted moments $\tilde{\mu}_n$ are derived from the integer moments μ_n as follows:

$$\tilde{\mu}_n = \sum_{k=0}^n (-1)^k \binom{n}{k} \bar{x}^k \mu_{n-k}, \quad n = 1, 2 \dots N_1 \leq N \quad (\text{A.7})$$

The shifted moments of the Beta KDF are calculated by:

$$\tilde{B}_n = \int_0^1 (x - \bar{x})^n K(x; x_i, h) dx \quad (\text{A.8})$$

Thus, the shifted moments $\tilde{\mu}_n^*$ of the reconstructed PDF are expressed as:

$$\tilde{\mu}_n^* = \sum_{i=0}^I \tilde{B}_{ni} p_i, \quad n = 1, 2 \dots N_1 \leq N \quad (\text{A.9})$$

The minimization problem (equation A.5) is reformulated as :

$$\left\| \begin{pmatrix} \mu_n \\ \tilde{\mu}_n \end{pmatrix} - \begin{pmatrix} B_n \\ \tilde{B}_n \end{pmatrix} p_I \right\|_{L^2} = \min, \quad \left(p_i \geq 0, \sum_{i=1}^I p_i = 1 \right) \quad (\text{A.10})$$

This new constraint minimization problem is numerically solved using NNLS or LSQLIN (Matlab sub-routines).

The algorithm of this method can be reduced to the following steps:

1. Define the reconstruction interval [a,b]
2. Transform the moments to the normalized interval [0,1]
3. Compute the shifted moments from the set of integer moments
4. Fix the number I of KDFs and the bandwidth parameter h
5. Compute the coefficients $B_{n,i}$ and $\tilde{B}_{n,i}$
6. Determine p_i by solving the constraint minimization problem (equation A.10)

Appendix A.2: Spline-based method

In order to optimize the reconstruction support and thus increase the accuracy of the spline-based method, the values of the reconstructed PDF $f^{(k)}(x)$ are checked at the boundaries of the support $[x_1^{(k)}, x_{n+1}^{(k)}]$ (i.e. in the subintervals $[x_1^{(k)}, x_2^{(k)}]$ and $[x_n^{(k)}, x_{n+1}^{(k)}]$). For this, these two subintervals are divided into 10 equidistant small subintervalls, the values of $f^{(k)}(x)$ at the nodes of these small subintervals are checked if they are sufficiently small against the maximal value of $f^{(k)}$ in order to reduce eventually the size of the reconstruction support. This test is given for the right boundary as (John et al., 2007):

$$\left(\sum_{j=1}^{10} \left[\left(f^{(k)}(x_{nj}) \right)^2 \right] + \left(f^{(k)}(x_{n+1}^{(k)}) \right)^2 \right)^{1/2} \leq tol_{red} f_{max}^{(k)} \quad (\text{A.11})$$

If equation A.11 is satisfied, the reconstruction support is reduced by setting $x_{n+1}^{(k+1)} = (x_n^{(k)} + x_{n+1}^{(k)})/2$, otherwise the boundary remains unchanged. For the new interval $[x_1^{(k+1)}, x_{n+1}^{(k+1)}]$, the nodes are redistributed equidistantly.

It is further checked that any value of $f^{(k)}(x)$ at the nodes $x_i (i = 1, \dots, n + 1)$ and at the midpoints of the subintervals are greater than a given tolerance tol_{neg} (equation A.12). This test is implemented to ensure the positivity of the PDFs.

$$f_{min,max} := \min_{j=1,\dots,k} f_{max}^{(j)}, \quad \frac{f^{(j)}(x_i)}{f_{min,max}} \geq tol_{neg}, \quad \frac{f^{(j)}(x_{i6})}{f_{min,max}} \geq tol_{neg} \quad (\text{A.12})$$

with $tol_{neg} \leq 0$. The problem of the ill-conditioning of the linear system of equations is treated by regulizing the system. This is achieved by neglecting small singular values according to a given tolerance tol_{sing} using a pseudo inverse routine of Matlab.

Note that in John et al. (2007), an equidistant grid is used for the distribution of the nodes x_i . This is not adapted for non-smooth and/or multimodal distributions. In the adaptive algorithm by (De Souza et al., 2010), this problem is solved by introducing a non-equidistant grid where the nodes are repositionned appropriately in order to capture accurately the PDF's critical domains.

This method is extensively described by John et al. (2007). The support of the target PDF $[a, b]$ is subdivided into n subintervals such as $a = x_1 < x_2 < \dots < x_{n+1} = b$. In each subinterval $[x_i, x_{i+1}]$, the target PDF is approximated by a piecewise polynomial $s^{(l)}(x)$ of degree l . The system of equations is detailed for cubic splines ($l = 3$). The unknowns are the four coefficients of the n splines. A smooth transition at the boundaries of the interval is assumed meaning that the PDF, its first and second derivatives are null at the boundaries, this gives 2×3 equations. The continuity of the splines, their first and second derivatives at the nodes provides $3(n - 1)$ equations. The remaining $(n - 3)$ equations are supplemented by the moments. This leads to solve a $4n \times 4n$ ill-conditioned linear system.

Since the set of the known moments limits the number of splines, one has to compute the reconstruction in the optimal support of $f(x)$ thus, the reconstruction is computed iteratively starting from an initial reconstruction $f^{(0)}(x)$ in an initial interval $[x_1^{(0)}, x_{n+1}^{(0)}]$.

In order to optimize the reconstruction support and thus increase the accuracy of the method, the values of the reconstructed PDF $f^{(k)}(x)$ are checked at the boundaries of the support $[x_1^{(k)}, x_{n+1}^{(k)}]$ (i.e. in the subintervals $[x_1^{(k)}, x_2^{(k)}]$ and $[x_n^{(k)}, x_{n+1}^{(k)}]$). For this, these two subintervals are divided into 10 equidistant small subintervals, the values of $f^{(k)}(x)$ at the nodes of these small subintervals are checked if they are sufficiently small against the maximal value of $f^{(k)}$ in order to reduce eventually the size of the reconstruction support. This test is given for the right boundary as (John et al., 2007):

$$\left(\sum_{j=1}^{10} \left[\left(f^{(k)}(x_{nj}) \right)^2 \right] + \left(f^{(k)}(x_{n+1}^{(k)}) \right)^2 \right)^{1/2} \leq tol_{red} f_{max}^{(k)} \quad (\text{A.13})$$

If equation A.13 is satisfied, the reconstruction support is reduced by setting $x_{n+1}^{(k+1)} = (x_n^{(k)} + x_{n+1}^{(k)})/2$, otherwise the boundary remains unchanged. For the new interval $[x_1^{(k+1)}, x_{n+1}^{(k+1)}]$, the nodes are redistributed equidistantly.

It is further checked that any value of $f^{(k)}(x)$ at the nodes $x_i (i = 1, \dots, n+1)$ and at the midpoints of the subintervals are greater than a given tolerance tol_{neg} (equation A.14). This test is implemented to ensure the positivity of the PDFs.

$$f_{min,max} := \min_{j=1,\dots,k} f_{max}^{(j)}, \quad \frac{f^{(j)}(x_i)}{f_{min,max}} \geq tol_{neg}, \quad \frac{f^{(j)}(x_{i6})}{f_{min,max}} \geq tol_{neg} \quad (\text{A.14})$$

with $tol_{neg} \leq 0$. The problem of the ill-conditioning of the linear system of equations is treated by regulizing the system. This is achieved by neglecting small singular values according to a given tolerance tol_{sing} using a pseudo inverse routine of Matlab.

Note that in John et al. (2007), an equidistant grid is used for the distribution of the nodes x_i . This is not adapted for non-smooth and/or multimodal distributions. In the adaptive algorithm by (De Souza et al., 2010), this problem is solved by introducing a non-equidistant grid where the nodes are repositionned appropriately in order to capture accurately the PDF's critical domains.

Appendix B: Analytical solution of the PBE in the case of breakage process

We give in this appendix the details for the analytical solution in its explicit form (equation 12).

By substituting equation 11 in 10, we obtain :

$$n(L, t) = \frac{1}{\sigma\sqrt{2\pi}} e^{-tL^2} \left(e^{-\frac{1}{2}\left(\frac{L-\mu}{\sigma}\right)^2} + 2t \int_L^\infty L' e^{-\frac{1}{2}\left(\frac{L'-\mu}{\sigma}\right)^2} dL' \right) \quad (\text{B.1})$$

We note I the integral term and proceed to the change of variable :

$$L' - \mu = \hat{L}' \mapsto L' = \hat{L}' + \mu \mapsto dL' = d\hat{L}' \quad (\text{B.2})$$

The integral term is written as:

$$I = \int \hat{L}' e^{-\frac{1}{2\sigma^2} \hat{L}'^2} d\hat{L}' + \mu \int e^{-\frac{1}{2\sigma^2} \hat{L}'^2} d\hat{L}' \quad (\text{B.3})$$

Recall that :

$$\int e^{-ax^2} dx = \frac{\sqrt{\pi}}{2\sqrt{a}} \operatorname{erf}(x\sqrt{a}) \quad (\text{B.4})$$

and

$$\int x e^{-ax^2} dx = -\frac{1}{2a} e^{-ax^2} \quad (\text{B.5})$$

Thus :

$$I = \sigma^2 e^{-\frac{1}{2}\left(\frac{L-\mu}{\sigma}\right)^2} + \mu\sigma\sqrt{\frac{\pi}{2}} \left(1 - \operatorname{erf}\left(\frac{1}{\sqrt{2}} \frac{L-\mu}{\sigma}\right)\right) \quad (\text{B.6})$$

430

By substituting equation B.6 in B.1, we obtain the final explicit solution given in equation 12.

Nomenclature

a, b	Lower and upper bounds of the reconstruction interval
B_n, \tilde{B}_n	Coefficients of the BKDF system of equations
$E(k)$	Global error function
$E_r(t)$	Mean absolute error for the reconstruction
$f(x)$	Probability Density Function
$f_M(x)$	The reconstructed Probability Density function
$g(x, \kappa, \lambda)$	Beta Probability Density Function
h	Bandwidth of the BKDF
$H[f]$	Shannon entropy
I	Number of BKDFs used for the reconstruction
k, n	moment's order
$K(x, x_*, h)$	Beta kernel density function
L, L'	Polymer chains length
L_i	Abscissae of the Gaussian quadrature
m	Mean of the normal law
M	Number of nodes of the Gaussian quadrature
$n(L, t)$	Length based number density function
N	Length of the set of moments
p_i	Weight coefficient, $\in [0, 1]$
q	Length of the discretized interval of reconstruction
t, t_i, t_f	Time, initial time, final time
w_i	Weights of the Gaussian quadrature
x	Variable of the PDF
\bar{x}	Parameter of the shifted moments, $\in [0, 1]$
x_*, x_i	Centers of the BKDFs

Greek Symbols

α	Factor of proportionality for the breakage frequency
β	Breakage kernel
γ	Breakage frequency
Γ	Gamma function
κ, λ	Parameters of the Beta Probability Density Function
μ	The set of moments
σ	Standard deviation for the normal law
ξ	Lagrange's multipliers

435 **Abbreviations**

BKDF	Beta Kernel Density Function
CFD	Computational Fluid Dynamics
CLD	Chain Length Distribution
DP	Degree of Polymerization
DQMOM	Direct Quadrature Method of Moments
KDF	Kernel Density Function
LQDMA	Long Quotient-Modified Difference Algorithm
LSQLIN	Constrained Linear Least Square
ME	Maximum Entropy
MWD	Molecular Weight Distribution
NNLS	Non-Negative Least Square
PBE	Population Balance Equation
PBM	Polupation Balance Modelling
PD	Product Difference Algorithm
PDF	Probability Density Function
QMOM	Quadrature Method of Moments

References

- Abramov, R. (2006). A practical computational framework for the multidimensional moment-constrained maximum entropy principle. *Journal of Computational Physics*, *211*, 198–209. URL: <http://www.sciencedirect.com/science/article/pii/S0021999105002688>. doi:10.1016/j.jcp.2005.05.008.
- 440 Abramov, R. V. (2007). An improved algorithm for the multidimensional moment-constrained maximum entropy problem. *Journal of Computational Physics*, *226*, 621–644. URL: <http://www.sciencedirect.com/science/article/pii/S0021999107001994>.
- Akhiezer, N. I. (1965). *The Classical Moment Problem: N.I. Akhiezer*. Oliver & Boyd.
- 445 Athanassoulis, G. A., & Gavriliadis, P. N. (2002). The truncated Hausdorff moment problem solved by using kernel density functions. *Probabilistic Engineering Mechanics*, *17*, 273–291. URL: <http://www.sciencedirect.com/science/article/pii/S0266892002000127>.
- Biswas, P., & Bhattacharya, A. K. (2010). Function reconstruction as a classical moment problem: a maximum entropy approach. *Journal of Physics A: Mathematical and Theoretical*, *43*, 405003. URL: <http://iopscience.iop.org/1751-8121/43/40/405003>. doi:10.1088/1751-8113/43/40/405003.
- 450 Bordás, R., John, V., Schmeier, E., & Thévenin, D. (2012). Numerical methods for the simulation of a coalescence-driven droplet size distribution. *Theoretical and Computational Fluid Dynamics*,

27, 253–271. URL: <http://link.springer.com/article/10.1007/s00162-012-0275-9>. doi:10.1007/s00162-012-0275-9.

455 Bose, S. M., & Git, Y. (2004). Mathematical modelling and computer simulation of linear polymer degradation: Simple scissions. *Macromolecular theory and simulations*, 13, 453–473. URL: <http://onlinelibrary.wiley.com/doi/10.1002/mats.200300036/full>.

De Souza, L. G. M., Janiga, G., John, V., & Thévenin, D. (2010). Reconstruction of a distribution from a finite number of moments with an adaptive spline-based algorithm. *Chemical Engineering Science*, 65, 2741–2750. URL: <http://www.sciencedirect.com/science/article/pii/S0009250910000163>.
460

Dette, H. (1997). *The Theory of Canonical Moments with Applications in Statistics, Probability, and Analysis*. John Wiley & Sons.

Diemer, R. B., & Olson, J. H. (2002). A moment methodology for coagulation and breakage problems: Part 2moment models and distribution reconstruction. *Chemical Engineering Science*, 57, 2211–2228. URL: <http://www.sciencedirect.com/science/article/pii/S0009250902001124>.
465

Gavriliadis, P. N., & Athanassoulis, G. A. (2003). Moment data can be analytically completed. *Probabilistic Engineering Mechanics*, 18, 329–338. URL: <http://www.sciencedirect.com/science/article/pii/S0266892003000468>. doi:10.1016/j.probengmech.2003.07.001.

Gavriliadis, P. N., & Athanassoulis, G. A. (2009). Moment information for probability distributions, without solving the moment problem, II: Main-mass, tails and shape approximation. *Journal of computational and applied mathematics*, 229, 7–15. URL: <http://www.sciencedirect.com/science/article/pii/S037704270800513X>.
470

Gavriliadis, P. N., & Athanassoulis, G. A. (2012). The truncated Stieltjes moment problem solved by using kernel density functions. *Journal of Computational and Applied Mathematics*, 236, 4193–4213. URL: <http://www.sciencedirect.com/science/article/pii/S0377042712002257>.
475

Gordon, R. G. (1968). Error Bounds in Equilibrium Statistical Mechanics. *Journal of Mathematical Physics*, 9, 655–663. URL: <http://scitation.aip.org/content/aip/journal/jmp/9/5/10.1063/1.1664624>. doi:10.1063/1.1664624.

Hackbusch, W., John, V., Khachatryan, A., & Suciu, C. (2012). A numerical method for the simulation of an aggregation-driven population balance system. *International Journal for Numerical Methods in Fluids*, 69, 1646–1660. URL: <http://onlinelibrary.wiley.com/doi/10.1002/flid.2656/abstract>. doi:10.1002/flid.2656.
480

Hulburt, H. M., & Katz, S. (1964). Some problems in particle technology: A statistical mechanical formulation. *Chemical Engineering Science*, 19, 555–574. URL: <http://www.sciencedirect.com/science/article/pii/0009250964850478>.
485

- John, V., Angelov, I., Öncül, A. A., & Thévenin, D. (2007). Techniques for the reconstruction of a distribution from a finite number of its moments. *Chemical Engineering Science*, *62*, 2890–2904. URL: <http://www.sciencedirect.com/science/article/pii/S0009250907002072>.
- John, V., & Thein, F. (2012). On the efficiency and robustness of the core routine of the quadrature method of moments (QMOM). *Chemical Engineering Science*, *75*, 327–333. URL: <http://www.sciencedirect.com/science/article/pii/S000925091200187X>. doi:10.1016/j.ces.2012.03.024.
- Kumar, S., & Ramkrishna, D. (1996). On the solution of population balance equations by discretization I. A fixed pivot technique. *Chemical Engineering Science*, *51*, 1311–1332. URL: <http://www.sciencedirect.com/science/article/pii/0009250996884892>. doi:10.1016/0009-2509(96)88489-2.
- Lebaz, N., Cockx, A., Spérandio, M., & Morchain, J. (2015). Population balance approach for the modelling of enzymatic hydrolysis of cellulose. *The Canadian Journal of Chemical Engineering*, *93*, 276–284. URL: <http://onlinelibrary.wiley.com/doi/10.1002/cjce.22088/abstract>. doi:10.1002/cjce.22088.
- Lee, K. W. (1983). Change of particle size distribution during Brownian coagulation. *Journal of Colloid and Interface Science*, *92*, 315–325. URL: <http://www.sciencedirect.com/science/article/pii/0021979783901534>.
- Lin, Y., Lee, K., & Matsoukas, T. (2002). Solution of the population balance equation using constant-number Monte Carlo. *Chemical Engineering Science*, *57*, 2241–2252. URL: <http://www.sciencedirect.com/science/article/pii/S0009250902001148>. doi:10.1016/S0009-2509(02)00114-8.
- Madras, G., & McCoy, B. J. (1998). Time evolution to similarity solutions for polymer degradation. *AIChE Journal*, *44*, 647–655. URL: <http://onlinelibrary.wiley.com/doi/10.1002/aic.690440313/abstract>. doi:10.1002/aic.690440313.
- Marchisio, D. L., & Fox, R. O. (2005). Solution of population balance equations using the direct quadrature method of moments. *Journal of Aerosol Science*, *36*, 43–73. URL: <http://www.sciencedirect.com/science/article/pii/S0021850204003052>.
- Marchisio, D. L., Pikturna, J. T., Fox, R. O., Vigil, R. D., & Barresi, A. A. (2003a). Quadrature method of moments for population-balance equations. *AIChE Journal*, *49*, 1266–1276. URL: <http://onlinelibrary.wiley.com/doi/10.1002/aic.690490517/abstract>.
- Marchisio, D. L., Vigil, R. D., & Fox, R. O. (2003b). Quadrature method of moments for aggregation-breakage processes. *Journal of Colloid and Interface Science*, *258*, 322–334. URL: <http://www.sciencedirect.com/science/article/pii/S0021979702000541>.
- Massot, M., Laurent, F., Kah, D., & De Chaisemartin, S. (2010). A robust moment method for evaluation of the disappearance rate of evaporating sprays. *SIAM Journal on Applied Mathematics*, *70*, 3203–3234. URL: <http://epubs.siam.org/doi/abs/10.1137/080740027>.

- McCoy, B. J., & Madras, G. (2001). Discrete and continuous models for polymerization and depolymerization. *Chemical Engineering Science*, *56*, 2831–2836. URL: <http://www.sciencedirect.com/science/article/pii/S0009250900005169>. doi:10.1016/S0009-2509(00)00516-9.
- McGraw, R. (1997). Description of Aerosol Dynamics by the Quadrature Method of Moments. *Aerosol Science and Technology*, *27*, 255–265. URL: <http://dx.doi.org/10.1080/02786829708965471>. doi:10.1080/02786829708965471.
- 525 Mead, L. R., & Papanicolaou, N. (1984). Maximum entropy in the problem of moments. *Journal of Mathematical Physics*, *25*, 2404–2417. URL: <http://scitation.aip.org/content/aip/journal/jmp/25/8/10.1063/1.526446>.
- Mortier, S. T. F., De Beer, T., Gernaey, K. V., & Nopens, I. (2014). Comparison of techniques for reconstruction of a distribution from moments in the context of a pharmaceutical drying process. *Computers & Chemical Engineering*, *65*, 1–8. URL: <http://www.sciencedirect.com/science/article/pii/S0098135414000404>.
- Ramkrishna, D., & Mahoney, A. W. (2002). Population balance modeling. Promise for the future. *Chemical Engineering Science*, *57*, 595–606. URL: <http://www.sciencedirect.com/science/article/pii/S0009250901003864>. doi:10.1016/S0009-2509(01)00386-4.
- 535 Shohat, J. A., & Tamarkin, J. D. (1943). *The Problem of Moments*. American Mathematical Soc.
- Tagliani, A. (1999). Hausdorff moment problem and maximum entropy: a unified approach. *Applied Mathematics and Computation*, *105*, 291–305. URL: <http://www.sciencedirect.com/science/article/pii/S009630039810084X>.
- Tagliani, A. (2001). Numerical aspects of finite Hausdorff moment problem by maximum entropy approach. *Applied mathematics and computation*, *118*, 133–149. URL: <http://www.sciencedirect.com/science/article/pii/S0096300399002106>.
- 540 Wheeler, J. C. (1974). Modified moments and Gaussian quadratures. *Rocky Mountain Journal of Mathematics*, *4*, 287–296. URL: <http://projecteuclid.org/euclid.rmjm/1250130972>.
- Yuan, C., Laurent, F., & Fox, R. O. (2012). An extended quadrature method of moments for population balance equations. *Journal of Aerosol Science*, *51*, 1–23. URL: <http://www.sciencedirect.com/science/article/pii/S0021850212000699>.
- 545 Ziff, R. M., & McGrady, E. D. (1985). The kinetics of cluster fragmentation and depolymerisation. *Journal of Physics A: Mathematical and General*, *18*, 3027. URL: <http://iopscience.iop.org/0305-4470/18/15/026>.